Critical Endpoint and Analytical Phase Diagram of Attractive Hard-Core Yukawa Spheres

Remco Tuinier[†,*] and Gerard J. Fleer[‡]

Forschungszentrum Jülich, Institut für Festkörperforschung, 52425 Jülich, Germany, and Laboratory of Physical Chemistry and Colloid Science, Wageningen University, 6703 HB Wageningen, The Netherlands

Received: June 12, 2006; In Final Form: August 18, 2006

We analytically calculate the gas−liquid critical endpoint (cep) for hard spheres with a Yukawa attraction. This cep is a boundary condition for the existence of a liquid. We use an analytical Helmholtz energy expression for the attractive Yukawa (hard) spheres based on the first-order mean spherical approximation to the attractive Yukawa potential by Tang and Lu (*J. Chem. Phys.* **1993**, *99*, 9828). This theory and our analytical simplification of it predict the gas−liquid and fluid−solid phase behavior, as found from computer simulations, very accurately as long as the range $1/\kappa$ of attraction is not too short. We find that the cep is situated at $\kappa\sigma \approx 6$ and at a contact potential around 2 *kT*. It follows that a liquid state is only possible when the attraction range is longer than $^1/_6$ of the particle diameter σ, and the attraction strength is smaller than 2 *kT*. The liquid region does not span more than 0.6 *kT* in strength, and there is also a relatively narrow window for the attraction range.

1. Introduction

The phase-diagram topology of atomic fluids as well as that of colloidal dispersions, including for instance protein solutions, is determined by the range of attraction with respect to the particle size.[1,2] Only if the range of attraction exceeds a certain value, gas−liquid (GL) coexistence is possible.[3−5] For a small range of attraction a GL phase transition is metastable.[1−7] Atoms of noble gases interact through a Lennard-Jones potential which is sufficiently long ranged to allow a GL transition so that, for example, helium liquefaction is possible.[5] In several protein solutions attractions are seemingly short ranged. Sometimes proteins are even simplified as sticky Baxter spheres,[8,9] and the observed liquid−liquid demixing is indeed often metastable with respect to gas−solid (GS),[10−12] in some cases preceding protein crystallization.[10,13]

The understanding of colloidal stability against demixing increased significantly since the development of the DLVO theory.[14,15] This theory describes the pair interaction between charged colloids as the sum of repulsive electrostatic and attractive dispersion contributions.[15,16] If the attraction is relatively strong, the colloidal dispersion becomes unstable. Commonly, in such dispersions the particles either percolate or agglomerate and sediment rather than phase separate. This is due to the fact that the relative range of attraction is rather small; usually it is less than 10% of the colloid radius for spheres with DLVO interaction. Such short-ranged attractions between hard-core particles can sometimes be described as sticky "Baxter" spheres with an infinitely deep and infinitely short-ranged attraction.[17] Computer simulations performed with a collection of Baxter spheres[18] demonstrate that percolation occurs either before or during a gas−liquid phase transition.

A systematic way to tailor the range of attraction is by adding nonadsorbing polymer to a stable dispersion of colloids.[19] The size of the polymer chains determines the range of attraction. Indeed, when the size of the polymer chains is sufficiently large with respect to the radius of the colloids, a colloidal GL phase transition can be induced.[20]

In this paper we systematically vary the range and strength of attraction to find the full phase behavior of a one-component system. As a simple model for the pair potential we use the attractive hard-core Yukawa interaction. The function that is nowadays termed Yukawa potential has a long history in physics and has been used in electrostatics and in theories of capillarity, fluids, and strong electrolytes[21] and has applications in soft matter systems such as colloidal dispersions.[22]

To describe a fluid of hard-core particles plus a Yukawa attraction, the mean spherical approximation (MSA) solution to the Ornstein−Zernike (OZ) equation[23] has often been used. A fully analytical but rather involved MSA solution in real space has been found by Waisman.[24] Expansions in terms of the contact potential up to fifth order were developed by Henderson et al.[25] Tavares and Prausnitz[26] used perturbation theory to compute fluid−fluid, fluid−solid, and solid−solid coexistence.

Tang and Lu[27] solved the OZ equation using MSA in Fourier and Laplace space and found that each perturbation term in the contact potential can be solved analytically. For the first-order expansion, termed FMSA, this leads to relatively simple and rather accurate solutions for the thermodynamic properties.[28,29]

In this paper we use FMSA and an even simpler analytical approximation to calculate the phase behavior of attractive hard-core Yukawa spheres. We consider both gas−liquid and fluid−solid coexistence. This allows us to calculate the gas−liquid critical endpoint[30] which identifies the boundary conditions for a stable liquid phase.

In the following sections we first review the FMSA theory in sections 2.1, 2.2, 2.3, and 2.4. Section 2.5 describes our simplification that allows to analytically calculate binodal curves. Subsequently, we compare the theory with computer simulation results (section 3.1) and present full phase diagrams (section 3.2), followed by a calculation of critical points, triple points, and an analysis of the *critical endpoint* (section 3.3).

2. Theory

2.1. Pair Potential and Free Energy Contributions. We consider a collection of hard-core spheres, with hard-core

* Corresponding author. E-mail: r.tuinier@fz-juelich.de.
[†] Forschungszentrum Jülich, Institut für Festkörperforschung.
[‡] Laboratory of Physical Chemistry and Colloid Science, Wageningen University.

10.1021/jp063650j CCC: $33.50
Published on Web 09/29/2006

diameter σ, plus a Yukawa attraction. The pair potential between two spheres can be written as

$$V(h) = \begin{cases} \infty & \text{for } h < 0 \\ -\dfrac{\epsilon}{1 + h/\sigma} \exp(-\kappa h) & \text{otherwise} \end{cases}, \quad (1)$$

where h equals $r - \sigma$, with r the center-to-center distance. The strength of the attraction is the contact potential $V(0) = \epsilon$ and the range is the screening length κ^{-1}. We define the relative range of attraction q (with respect to the particle radius $\sigma/2$) as $\kappa^{-1}/(\sigma/2) = 2/\kappa\sigma$.

We focus on the Helmholtz energy density $f = \beta\upsilon F/V$, where $\upsilon = \pi\sigma^3/6$ is the volume of a sphere, $\beta = 1/kT$, F the Helmholtz energy, and V the volume of the system. The quantity f is written as

$$f = f_0 + f_a = f_{id} + f_0^{ex} + f_a \quad (2)$$

where f is split into a hard-sphere contribution f_0 and an attractive contribution f_a. In turn, the hard-sphere part f_0 can be split into an ideal-gas contribution f_{id} and a many-body excess part f_0^{ex}. In the classical van der Waals treatment f_a equals $-\gamma\phi^2$, where ϕ is the volume fraction of the spheres and γ is a constant that characterizes the attractions.

2.2. Hard-Sphere Contributions. The ideal-gas contribution f_{id} is given by

$$f_{id} = \phi \ln \phi - \phi + \phi \ln \Lambda^3/\upsilon \quad (3)$$

where Λ is the thermal de Broglie wavelength.

For the excess part of a fluid, we start from the Carnahan−Starling[31] expression for the (osmotic) pressure Π_0, which is rather accurate

$$\Pi_0\upsilon\,(\text{fluid}) = \frac{\phi + \phi^2 + \phi^3 - \phi^4}{(1 - \phi)^3} \quad (4)$$

where $\Pi_0\upsilon$ is in units kT. From the Gibbs−Duhem relation $\partial\Pi\upsilon/\partial\phi = \phi\partial\mu/\partial\phi$ (at fixed temperature), one obtains the chemical potential (also in kT units)

$$\mu_0\,(\text{fluid}) = \ln(\phi\Lambda^3/\upsilon) + \frac{8\phi - 9\phi^2 + 3\phi^3}{(1 - \phi)^3} \quad (5)$$

where the first term is the ideal contribution $\mu_{id} = \partial f_{id}/\partial\phi$. The excess free energy now follows from $f = \phi\mu - \Pi\upsilon$

$$f_0^{ex}\,(\text{fluid}) = \frac{4\phi^2 - 3\phi^3}{(1 - \phi)^2} \quad (6)$$

For a crystal phase with a face-centered-cubic (fcc) arrangement, we use the expression of Hall[32] for the osmotic pressure

$$\Pi_0\upsilon\,(\text{crystal}) = \frac{3\phi}{1 - \phi/\phi_{cp}} \quad (7)$$

where $\phi_{cp} = \pi 2^{1/2}/6 \approx 0.74$ is the volume fraction at close packing. We also need the chemical potential of the crystal, which follows again from the Gibbs−Duhem relation as above

$$\mu_0\,(\text{crystal}) = \ln(\phi\Lambda^3/\upsilon) + 2.1306 + \frac{3}{1 - \phi/\phi_{cp}} + 3\ln\left[\frac{\phi}{1 - \phi/\phi_{cp}}\right] \quad (8)$$

The numerical constant 2.1306 is derived from computer simulation results.[33] Hence the expression for the excess Helmholtz energy density is

$$f_0\,(\text{crystal}) = \phi \ln(\phi\Lambda^3/\upsilon) + \phi\left(2.1306 + 3\ln\left[\frac{\phi}{1 - \phi/\phi_{cp}}\right]\right) \quad (9)$$

2.3. FMSA Theory. We briefly review the relevant expressions for the attractive part f_a according to the first-order mean spherical approximation (FMSA) by Tang et al.[27−29] Previously, it has been shown that FMSA predicts the equation of state very accurately.[28,29]

Tang et al.[29] derived an expression for f_a that can be written in the van der Waals form

$$f_a = -\gamma\phi^2 \quad (10)$$

where γ, in contrast with the van der Waals parameter, depends on the volume fraction and can be split into two terms: $\gamma = \gamma_1\beta\epsilon + \gamma_2(\beta\epsilon)^2$, where γ_1 and γ_2 are given by

$$\gamma_1(\phi) = 3\frac{q^2 L(\phi)}{(1 - \phi)^2[1 + Q(\phi)]} \quad (11)$$

$$\gamma_2(\phi) = \frac{3q}{2[1 + Q(\phi)]^4} \quad (12)$$

The functions L and Q are

$$L(\phi) = 1 + \frac{2}{q} + \phi\left(2 + \frac{1}{q}\right) \quad (13)$$

$$Q(\phi) = \frac{6\phi(1 - \phi)q + 9\phi^2q^2 - 3\phi q^3[1 + 2\phi + L(\phi)\exp(-2/q)]}{2(1 - \phi)^2} \quad (14)$$

2.4. Phase Coexistence. Coexisting concentrations can now be computed from equal osmotic pressure Π and chemical potential μ in both phases. These quantities follow straightforwardly from f as $\beta\Pi\upsilon = \phi\partial f/\partial\phi - f$ and $\beta\mu = \partial f/\partial\phi$. For GL coexistence we have

$$\mu(\phi_G) \equiv \mu(\phi_L) \quad (15)$$

$$\Pi(\phi_G) \equiv \Pi(\phi_L) \quad (16)$$

with eqs 4 and 5 for Π_0 and μ_0, respectively. For FS coexistence we analogously use

$$\mu(\phi_F) \equiv \mu(\phi_S) \quad (17)$$

$$\Pi(\phi_F) \equiv \Pi(\phi_S) \quad (18)$$

with eqs 4 and 5 for Π_0 and μ_0 on the left-hand fluid side and eqs 7 and 8 for Π_0 and μ_0 on the right-hand crystal side. We assume that the attraction in the concentrated crystal phases is still described by eq 10, which is a result derived for a fluid. This assumption seems appropriate for other types of attractions (see ref 6 for depletion attractions) and the approximation is probably reasonable because the hard core contribution f_0 dominates for such a highly concentrated phase.

2.5. Analytical Approximation. Close inspection of expressions 11 and 12 for γ_1 and γ_2 to γ in eq 10 shows that $\gamma_1\beta\epsilon$ dominates. Neglecting $\gamma_2(\beta\epsilon)^2$ we can write

$$f = f_0 - \beta\epsilon G(\phi) \tag{19}$$

with a simple volume-fraction-dependent function $G(\phi)$

$$G(\phi) = \phi^2 \frac{a_0 + a_1\phi}{b_0 + b_1\phi + b_2\phi^2} \tag{20}$$

The coefficients a_i and b_i depend only on the relative range of the Yukawa potential q. They are expressed most easily in its inverse $k = 1/q = \kappa\sigma/2$

$$a_0 = 4k^2 + 2k$$

$$a_1 = 2k^2 + 4k \tag{21}$$

$$b_0 = \frac{2k^3}{3}$$

$$b_1 = \chi_1 - \frac{4k^3}{3} + 2k^2 - 1 \tag{22}$$

$$b_2 = \chi_2 + \frac{2k^3}{3} - 2k^2 + 3k - 2$$

where χ_1 and χ_2 are defined as

$$\chi_1 = (2k + 1)\exp(-2k)$$

$$\chi_2 = (k + 2)\exp(-2k) \tag{23}$$

We note that a volume-fraction-independent γ survives in the low ϕ limit, for which G becomes $3q(2 + q)\phi^2$, so $\gamma = -3\beta\epsilon q(2 + q)$. However, in very concentrated systems G becomes proportional to ϕ.

An analytical expression for the chemical potential is obtained from $\mu = \partial f/\partial\phi$

$$\mu = \mu_0 - \beta\epsilon H(\phi) \tag{24}$$

where $H(\phi)$ is given by

$$H(\phi) = \phi \frac{c_0 + c_1\phi + c_2\phi^2 + c_3\phi^3}{(b_0 + b_1\phi + b_2\phi^2)^2} \tag{25}$$

with the following q-dependent coefficients:

$$c_0 = 2a_0b_0$$

$$c_1 = a_0b_1 + 3a_1b_0 \tag{26}$$

$$c_2 = 2a_1b_1$$

$$c_3 = a_1b_2$$

The (osmotic) pressure follows from $\Pi v = \phi\mu - f$

$$\Pi v = \Pi_0 v + \epsilon J(\phi) \tag{27}$$

with $J(\phi)$ given by

$$J(\phi) = G(\phi) - \phi H(\phi) \tag{28}$$

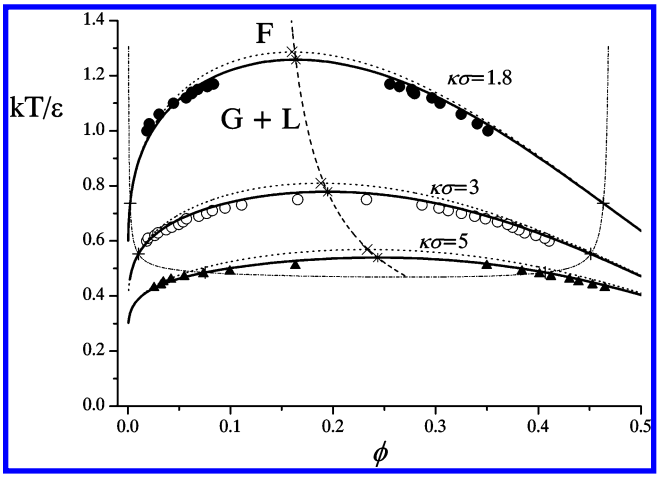

Figure 1. Gas−liquid coexistence of a collection of hard-core attractive Yukawa spheres. Symbols are simulation results,[34] the solid curves are FMSA,[29] the dotted curves are our analytical simplification. Pluses identify the triple points and dot−dashed curves connect them for a wide range of $\kappa\sigma$'s. Crosses and asterisks represent the theoretical critical points. The dashed curve gives the FMSA critical line. Capital letters refer to $\kappa\sigma = 1.8$.

We now have analytical expressions for both μ and Π. To calculate the GL binodal, we eliminate ϵ from eqs 15 and 16 to find the analytical coexistence relation

$$\epsilon = \frac{\mu_0^{\mathrm{L}}(\phi_{\mathrm{L}}) - \mu_0^{\mathrm{G}}(\phi_{\mathrm{G}})}{H(\phi_{\mathrm{L}}) - H(\phi_{\mathrm{G}})} = \frac{\Pi_0^{\mathrm{L}}(\phi_{\mathrm{L}})v - \Pi_0^{\mathrm{G}}(\phi_{\mathrm{G}})v}{J(\phi_{\mathrm{L}}) - J(\phi_{\mathrm{G}})} \tag{29}$$

For both μ_0^{G} and μ_0^{L} we use eq 5, and for both Π_0^{G} and Π_0^{L} we use eq 4. For a given q the second and third parts of this equation relate the volume fractions at coexistence. We choose a value for ϕ_{G}, and the corresponding ϕ_{L} is solved using the second equality of eq 29. The first equality then tells to which Yukawa contact potential ϵ those binodal concentrations correspond. We note that the calculation of binodals in the analytical model involves nothing more than solving one equation in one unknown.

For FS coexistence we obtain analogously

$$\epsilon = \frac{\mu_0^{\mathrm{S}}(\phi_{\mathrm{S}}) - \mu_0^{\mathrm{F}}(\phi_{\mathrm{F}})}{H(\phi_{\mathrm{S}}) - H(\phi_{\mathrm{F}})} = \frac{\Pi_0^{\mathrm{S}}(\phi_{\mathrm{S}})v - \Pi_0^{\mathrm{F}}(\phi_{\mathrm{F}})v}{J(\phi_{\mathrm{S}}) - J(\phi_{\mathrm{F}})} \tag{30}$$

In this case we use μ_0^{S} from eq 8 and Π_0^{S} from eq 7. As in eq 29, the fluid parts are obtained from eqs 4 and 5.

3. Results

3.1. Comparison of Theory with Computer Simulations. In this section we compare the results of the predicted binodal curves for the theories outlined in sections 2.3 and 2.5 with computer simulation results.

In Figure 1 we plotted results for the GL coexistence for $\kappa\sigma = 1.8$, 3, and 5 (corresponding to q values of 1.11, 0.67, and 0.4). The data points are computer simulation data from Shukla,[34] who performed Gibbs ensemble Monte Carlo simulations on a collection of spheres interacting through a potential V given in eq 1. The full curves were calculated using the full FMSA theory (eq 2 plus eq 10). It is clear that FMSA describes the computer simulation data excellently. We calculate the critical point using $\mathrm{d}^3f/\mathrm{d}\phi^3 = \mathrm{d}^2f/\mathrm{d}\phi^2 \equiv 0$ or $\mathrm{d}^2\Pi/\mathrm{d}\phi^2 = \mathrm{d}\Pi/\mathrm{d}\phi \equiv 0$. The crosses at the top of the curves identify the critical points that follow from FMSA theory. We cannot compare these critical points with simulation data; Gibbs-ensemble MC

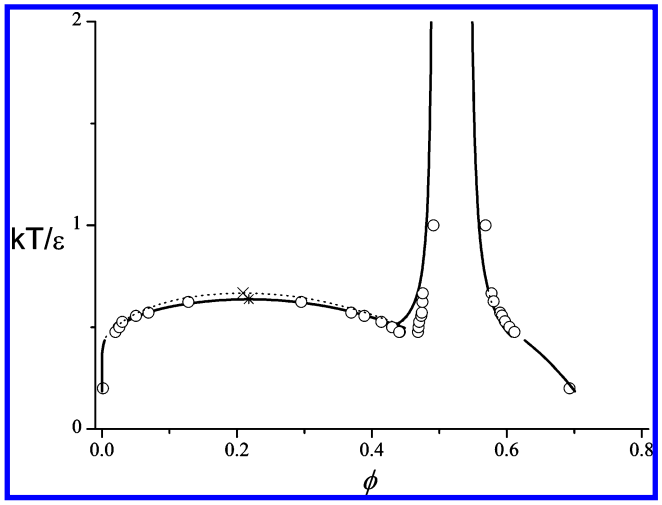

Figure 2. Phase behavior of a dispersion of spherical hard-core attractive Yukawa particles with $\kappa\sigma = 3.9$. Symbols are simulation results,[7] the solid curves are FMSA,[29] the dotted curves are our analytical simplification. Cross and asterisk are critical points, and pluses identify the three coexisting phases of the triple points. The three pluses are connected through a thin line.

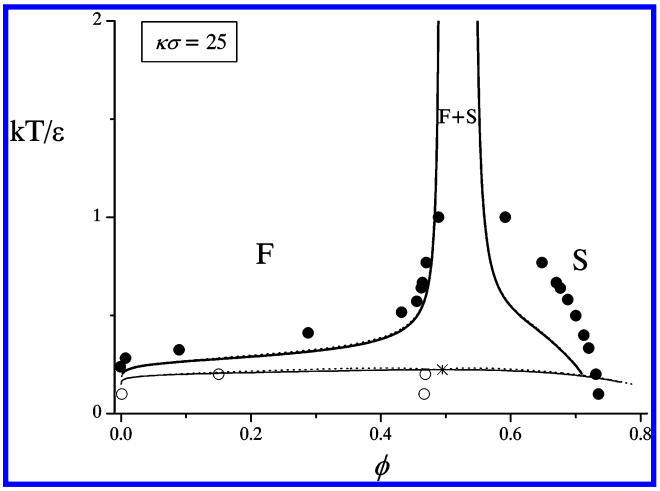

Figure 3. As Figure 2 but for $\kappa\sigma = 25$. The GL coexistence is now metastable, and there is no triple point.

simulations near the critical point are only accurate for very large simulation boxes. Guided by the binodal simulation points, it seems that the critical point is predicted quite accurately.

The dotted curves are the analytical results for the GL binodals according to eq 29. These predictions are very close to the full FMSA and the computer simulation results. The analytical results lie slightly above the FMSA and simulation data in terms of kT/ϵ. Despite the simplicity of the equations, the analytical approximation is capable of describing GL phase behavior accurately, and thus the model could be helpful for, e.g., engineering purposes. Shukla[34] already showed that the full MSA results of Henderson et al.,[25] which are much more involved numerically than the FMSA approach,[28] describe the simulation results very well. The difference between FMSA, our simple analytical approximation and the full MSA by Henderson et al.[25] is hardly perceptible. The numerical effort, however, is reduced tremendously in our model. We note that the predictions of Tavares and Prausnitz,[26] which require quite some numerical effort, predict less accurate binodals.

Calculating only GL binodals does not tell us whether the coexistence curves are stable or metastable, so it is not sufficient to predict whether a stable liquid can be formed. To that end we need the triple points, in which also the fluid−solid equilibrium is taken into account. Triple points are calculated from eqs 31 and 32 below. We have indicated in Figure 1 the (analytical) FMSA results (pluses) for the G and L compositions of the triple point for the three $\kappa\sigma$ values. Only the part of the GL coexistence curve between the pluses is stable. The dot−dash curve connecting the pluses gives the triple curve for a wide range of $\kappa\sigma$'s. The dashed curve connects the GL critical points.

There are also simulation data for gas−liquid plus fluid−solid and gas−solid coexistence. These give the opportunity to test the accuracy of our analytical predictions. Dijkstra[7] performed MC computer simulation results of spheres that interact through the attractive Yukawa potential of eq 1, for $\kappa\sigma = 3.9$ and 25, corresponding to a relative range of attraction q of 0.51 and 0.08, respectively. We plot the results in Figures 2 and 3 (circles), together with the full FMSA (solid curves) and our analytical approximation (dotted).

We first focus on Figure 2 ($\kappa\sigma = 3.9$). For weak attractions (large kT/ϵ) only FS coexistence occurs, as for hard spheres without attractions. The coexistence concentrations are also about the same. For example, for $kT/\epsilon = 2$ they are $\phi_F = 0.488$ and $\phi_S = 0.549$, which is rather close to the FS transition concentrations of hard spheres at $\phi_F = 0.494$ and $\phi_S = 0.545$. Upon increase of the contact potential (lowering kT/ϵ), the FS coexistence region slightly widens until it meets the GL coexistence region at the triple point. The fluid is stable in a narrow range of kT/ϵ, roughly $0.64 < kT/\epsilon < 0.51$, where the first number corresponds to the critical point and the second to the triple point. The analytical results for the critical point (cross) and triple point (pluses) are indicated. For stronger attraction ($kT/\epsilon < 0.5$) there is only GS demixing, with a very dilute gas phase and a very concentrated solid. In Figure 2 there is nearly quantitative agreement between theory and simulations.

Figure 3 gives the results for $\kappa\sigma = 25$. The GL curve now lies below the FS curve, so the entire GL binodal curve is metastable. Therefore, there is no triple point in this case. Both FMSA theory (solid curves) as well as our analytical approximation (dotted curve) describe the GL simulation data (open circles) very well. For the FS coexistence (closed circles) we see that the fluid side of the binodal curve is predicted reasonably well by (analytical) FMSA, but the solid side is inaccurate. We conclude that eq 10 is a good approximation for sufficiently long-ranged attractions, but it leads to deviations for short-ranged interactions, especially at the solid side of the coexistence curves. We recall that FMSA is based on an expansion in $\beta\epsilon$, so we cannot expect that this theory is accurate for small values of kT/ϵ. From a comparison of various thermodynamic computer simulation data it seems that FMSA is accurate for $\kappa\sigma < 8$,[29] which is confirmed by our analysis above.

3.2. Full Phase Diagrams. In Figure 4 we plot coexistence curves calculated using FMSA (the analytical approximation hardly differs) for a few indicative $\kappa\sigma$ values: 4, 6.32, 10, and 20. We shall show that $(\kappa\sigma)^* = 6.32$ corresponds to the critical endpoint (cep). We plot now $\beta\epsilon$ along the ordinate axis, and use $y = \phi/(1 - \phi)$ as concentration variable because it makes the curves on the fluid side more symmetrical. For $\kappa\sigma$ values of 20 and 10, we find only fluid−solid coexistence (solid curves). In the absence of attractions ($\epsilon = 0$) fluid−solid coexistence occurs at the pure hard spheres concentrations of $\phi = 0.49$ ($y = 0.97$) and $\phi = 0.54$ ($y = 1.18$). With increase in ϵ, the fluid−solid transition widens, an effect that becomes more pronounced for longer-ranged attractions (smaller $\kappa\sigma$). For $\kappa\sigma = 20$ and 10, fluid−fluid or gas−liquid demixing is metastable

and takes place only for large $\beta\epsilon$ (4.0 and 2.7, respectively); this metastable region is not shown in Figure 4. The dashed curve indicates the stable gas−liquid binodal for $\kappa\sigma = 4$; the open circle at its lowest point is the critical point for this $\kappa\sigma$. We indicated stable critical points (open circles) for 10 values of $\kappa\sigma$ (see legend). The curve that connects these points is the critical line, which at the top ends in the critical endpoint at $\kappa\sigma = 6.32$. For the same range of $\kappa\sigma$'s we plotted the triple points (closed circles) at which gas, liquid, and solid coexist. The triple points are connected through the dotted curve; obviously, it has three branches. The cep is the highest point of the triple curve; at that point the gas−liquid coexistence point is critical *and* is in equilibrium with a solid phase. We also drew the fluid−solid binodal at $\kappa\sigma = 6.32$; the fluid branch has an inflection point with zero slope of the curve in the cep. The cep thus indicates the transition from a stable to an unstable gas−liquid coexistence region.

3.3. Critical Endpoint. We now investigate under which conditions a stable liquid of hard-core attractive Yukawa spheres exists. To do so we need the gas−liquid critical endpoint (cep), where the gas−liquid critical point coincides with the gas−liquid−solid triple point. For any $q > q^*$ or $\kappa\sigma < \kappa\sigma^*$, the triple point is calculated from the following condition

$$\mu(\phi_G) \equiv \mu(\phi_L) \equiv \mu(\phi_S) \tag{31}$$

$$\Pi(\phi_G) \equiv \Pi(\phi_L) \equiv \Pi(\phi_S) \tag{32}$$

which was used to calculate the filled circles in Figure 4. For given q, eqs 31 and 32 constitute a set of four equations in four unknowns (ϵ^t and three concentrations ϕ_g^t, ϕ_l^t, and ϕ_s^t). For our analytical model, where ϵ can be eliminated, the equations can be manipulated such that only one equation in one unknown is solved at the same time.

In the critical endpoint a solid phase coexists with a *critical* fluid phase, so we have the conditions for a critical point supplemented with equal μ and Π in fluid and solid phases.

$$\mu(\phi_F) \equiv \mu(\phi_S)$$

$$\Pi(\phi_F) \equiv \Pi(\phi_S) \tag{33}$$

$$\frac{d^2\Pi(\phi_F)}{d\phi_F^{\,2}} = \frac{d\Pi(\phi_F)}{d\phi_F} \equiv 0$$

Again FMSA requires solving four equations in four unknowns, which in the analytical model can be reduced to one equation in one unknown. In FMSA the critical endpoint is

$$(\phi_F)^* = 0.272 \quad (\phi_S)^* = 0.619 \tag{34}$$

$$(\beta\epsilon)^* = 2.133 \quad (\kappa\sigma)^* = 6.320 \tag{35}$$

and with our analytical approximation we find

$$(\phi_F)^* = 0.272 \quad (\phi_S)^* = 0.621 \tag{36}$$

$$(\beta\epsilon)^* = 2.119 \quad (\kappa\sigma)^* = 6.920 \tag{37}$$

The two sets of data are nearly the same, except for $(\kappa\sigma)^*$ where there is a slight difference. We note that $(\kappa\sigma)^*$ corresponds to a relative range $q^* = 0.32$ (FMSA) or $q^* = 0.29$ (analytical): the minimum range for which liquid exists is roughly one-third of the particle radius. The cep indicates the boundary condition for a stable liquid; the contact potential should be smaller than

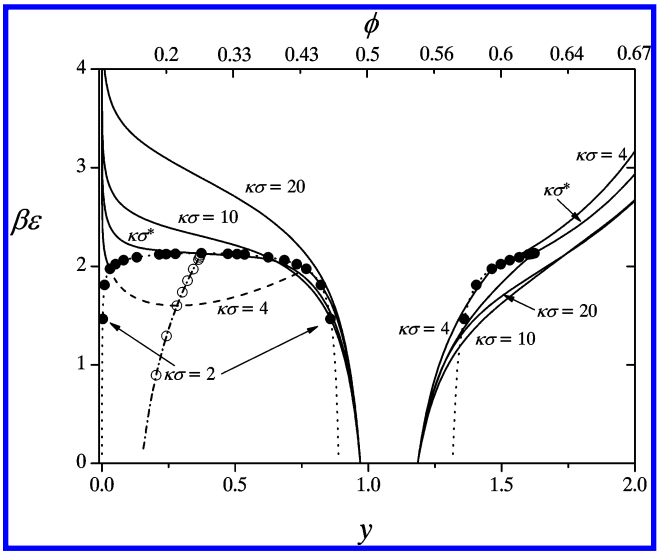

Figure 4. Binodal curves from FMSA theory for an attractive range $\kappa\sigma = 20$, 10, and 4, and $(\kappa\sigma)^* = 6.32$ (which corresponds to the cep). The lower horizontal axis is $y = \phi/(1 - \phi)$. Solid curves are FS binodals, the dashed curve is the GL binodal for $\kappa\sigma = 4$. Symbols indicate the triple (filled circles) and critical (open circles) points for $\kappa\sigma = 2$ (indicated), 3, 4, 4.5, 5, 5.5, 6, 6.1, 6.2, and 6.32; the curves connecting these points are the critical curve (dot−dashed) and the triple curve (dotted). The point where the critical and triple curves meet is the fluid part of the cep; its coordinates are $\beta\epsilon = 2.133$ and $y_F^* = 0.374$. The solid part of the cep is at $y_S^* = 1.625$.

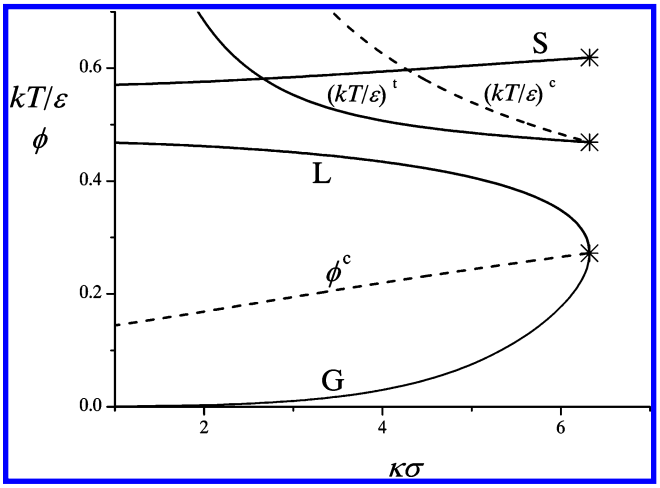

Figure 5. Triple (solid) and critical (dashed) curves as a function of the (inverse) range of attraction $\kappa\sigma$. The volume fractions of gas, liquid, and solid at the triple points are indicated by G, L, and S along the curves. The symbol ϕ^c indicates the critical volume fraction for various $\kappa\sigma$ values. The (inverse) contact potentials $\beta\epsilon$ at the critical and triple points are indicated using the superscripts c and t. The cep values are indicated by the asterisks.

2.1 kT and $\kappa\sigma$ should be smaller than 6.3 (we assume FMSA to be more accurate here). The value of q^* agrees with results for the depletion-induced attractions between hard spheres due to nonadsorbing polymer chains[3,6] and to results for particles interacting through a Lennard-Jones-like potential.[35] The coordinates of the critical endpoint thus seem to be independent of the details of the contact potential in the case of a potential consisting of a hard core plus a smooth attractive contribution.

In Figure 5 we plot the triple (solid curves) and critical (dashed) volume fractions (G, L, and S and ϕ^c) and the (inverse) contact potentials in triple and critical points as a function of $\kappa\sigma$. Asterisks denote the cep. Just below the cep the gas and liquid concentrations at the triple point change rapidly while

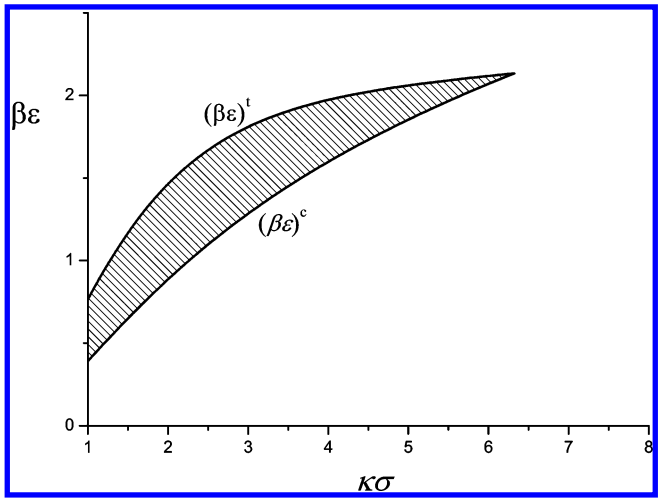

Figure 6. Liquid window indicating for which combination of contact potentials and relative range of attraction a stable liquid can be formed as a function of the range of attraction, characterized by $\kappa\sigma$. The window in ϵ is about 0.5 kT for $\kappa\sigma < 4$. The window in $\kappa\sigma$ is about 1.7 for $\beta\epsilon = 1.5$ and is smaller for larger and smaller $\kappa\sigma$ values. The cep value is indicated by the asterisk.

the concentration of the solid phase does not vary much. With increase in the range of attraction, the volume fraction at the critical point decreases. The contact potentials at the triple and critical point both decrease with increasing range of the attraction, which tells us that a stable liquid above $(\beta\epsilon)^*$ does not exist. Only between $(\beta\epsilon)^t$ and $(\beta\epsilon)^c$ is a stable liquid possible. The latter feature is more easily shown by replotting the kT/ϵ curves in Figure 5 as its inverse $\beta\epsilon$. In Figure 6 we did this, and we show the liquid window as the hatched region. This region is rather small and does not exceed 0.6 kT in ϵ and at most 1.5 in $\kappa\sigma$. The maximum range in ϵ is around $\kappa\sigma = 2$, the maximum range in $\kappa\sigma$ is around $\beta\epsilon = 1.5$. These numbers indicate how subtle the liquid state for a single-component system is.

Even when the suitable range of attraction ($\kappa\sigma < 6$) is achieved, there is only a tiny range of attraction strengths for which a liquid exists. For too strong an attraction only fluid−solid coexistence occurs, for too weak an attraction only gas−solid coexistence is found. Conversely, when we have the appropriate strength ($\epsilon < 2\ kT$), there is only a limited window for the relative attraction range: $q = {}^1/_3$ is the minimum, but for smaller ϵ the q-window should be in the narrow range between critical point and triple point for liquid to be stable. For example, for $\epsilon = 1.5\ kT$ the q-window is between 0.5 and 0.8.

This subtle balance is less critical when a second component is used to induce attractions by means of a depletion interaction.[19] In that case many-body interactions increase the liquid window.

4. Conclusions

We reformulate the first-order mean spherical approximation (FMSA) and can then calculate the Helmholtz energy of both fluid and solid states of hard spheres with a Yukawa attraction. Both the strength and the range of the attraction can be varied. This allows accurate computation of gas−liquid and fluid−solid binodals for such particles. Excellent agreement is found with computer simulation results when the range of attraction is not too short. For higher ranges the agreement is no longer quantitative, but the trends are still correctly described. A simplification of the theory allows an analytical calculation of binodal curves; the results are very close to the full FMSA. We computed also analytically fluid−fluid critical points and triple points where gas, liquid, and solid coexist. The point where the critical curve and the triple curve meet is the gas−liquid critical endpoint (cep), which defines the border at which a liquid can exist. This cep corresponds to a range of attraction which is one-third of the hard-sphere radius, and an attractive contact potential of 2 kT. We analyze the liquid window and find it is narrow; it is between 0 and 0.6 kT in attraction strength and is also narrow in the range of potential at given strength. Hence, the existence of a liquid state is very subtle in a one-component system. A very specific combination of range and strength of attraction is required for a stable liquid.

Acknowledgment. We thank Dr. Marjolein Dijkstra for providing us with her computer simulation data and Mieke Tuinier-Kröner for preparing part of the manuscript. Christoph Gögelein is acknowledged for a critical reading of the manuscript.

References and Notes

(1) Poon, W. C. K.; Pusey, P. N.; Lekkerkerker, H. N. W. *Phys. World* **1996**, *April*, 27.
(2) Lekkerkerker, H. N. W. *Physica A* **1997**, *244*, 227.
(3) Gast, A. P.; Hall, C. K.; Russel, W. B. *J. Colloid Interface Sci.* **1983**, *96*, 251.
(4) Tejero, C. F.; Daanoun, A.; Lekkerkerker, H. N. W.; Baus, M. *Phys. Rev. Lett.* **1994**, *73*, 752.
(5) Hasegawa, M.; Ohno, K. *J. Phys.*: *Condens. Matter* **1997**, *9*, 3361.
(6) Lekkerkerker, H. N. W.; Poon, W. C. K.; Pusey, P. N.; Stroobants, A.; Warren, P. B. *Europhys. Lett.* **1992**, *20*, 559.
(7) Dijkstra, M. *Phys. Rev. E* **2002**, *66*, 021402.
(8) de Kruif, C. G. *Langmuir* **1992**, *8*, 2932.
(9) Piazza, R.; Peyre, V.; Digiorgio, V. *Phys. Rev. E* **1998**, *58*, R2733.
(10) Muschol, M.; Rosenberger, F. *J. Chem. Phys.* **1997**, *107*, 1953.
(11) Annunziata, O.; Asherie, N.; Lomakin, A.; Pande, J.; Ogun, O.; Benedek, G. B. *Proc. Natl. Acad. Sci. U.S.A.* **2002**, *99*, 14165.
(12) Poon, W. C. K. *Phys. Rev. E* **1997**, *55*, 003762.
(13) Ten Wolde, P. R.; Frenkel, D. *Science* **1995**, *277*, 1975.
(14) Deryagin, B. V.; Landau, L. *Acta Physicochim. U.R.S.S.* **1941**, *14*, 633.
(15) Verwey, E. J. W.; Overbeek, J. Th. *Theory of the Stability of Lyophobic Colloids*; Elsevier: Amsterdam, 1948.
(16) Russel, W. B.; Saville, D. A.; Schowalter, W. R. *Colloidal Dispersions*; Cambridge Universtity Press: New York, 1989.
(17) Baxter, R. J. *J. Chem. Phys.* **1968**, *49*, 2770.
(18) Miller, M. A.; Frenkel, D. *J. Chem. Phys.* **2004**, *121*, 535.
(19) Poon, W. C. K. *J. Phys: Condens. Matter* **2002**, *14*, R859.
(20) Ilett, S. M.; Orrock, A.; Poon, W. C. K.; Pusey, P. N. *Phys. Rev. E* **1995**, *51*, 1344.
(21) Rowlinson, J. S. *Physica A* **1989**, *156*, 15.
(22) Bergenholtz, J.; Fuchs, M. *Phys. Rev. E* **1999**, *59*, 5706.
(23) Hansen, J.-P.; McDonald, I. R. *Theory of Simple Liquids*; Academic Press: San Diego, CA, 1986.
(24) Waisman, E. *Mol. Phys.* **1973**, *25*, 45.
(25) Henderson, D.; Blum, L.; Noworyta, J. P. *J. Chem. Phys.* **1995**, *102*, 4973.
(26) Tavares, F. W.; Prausnitz, J. M. *Colloid Polym. Sci.* **2004**, *282*, 620.
(27) Tang, Y.; Lu, B. C.-Y. *J. Chem. Phys.* **1993**, *99*, 9828.
(28) Tang, Y. *J. Chem. Phys.* **2003**, *118*, 4140.
(29) Tang, Y.; Lin, Y.-Z.; Li, Y.-G. *J. Chem. Phys.* **2005**, *122*, 184505.
(30) Rowlinson, J. S.; Widom, B. *Molecular theory of capillarity*; Clarendon: Oxford, 1982.
(31) Carnahan, N. F.; Starling, K. E. *J. Phys. Chem.* **1969**, *51*, 635.
(32) Hall, C. K. *J. Chem. Phys.* **1972**, *52*, 2252.
(33) Frenkel, D.; Ladd, A. J. C. *J. Chem. Phys.* **1984**, *81*, 3188.
(34) Shukla, K. P. *J. Chem. Phys.* **2000**, *112*, 10358.
(35) Vliegenthart, G. A.; Lodge, J. F. M.; Lekkerkerker, H. N. W. *Physica A* **1999**, *263*, 378.